

# Cleavage Reactions of Radical Anions that Range from Homolytic to Heterolytic within the Same Family of Compounds

Zi-Rong Zheng,<sup>1a</sup> Dennis H. Evans,<sup>\*,1a</sup> Elisa Soazara Chan-Shing,<sup>1b</sup> and Jean Lessard<sup>1b</sup>

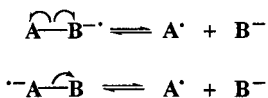
Contribution from the Department of Chemistry and Biochemistry, University of Delaware, Newark, Delaware 19706, and Centre de Recherche en Electrochimie et Electrocatalyse, Département de Chimie, Université de Sherbrooke, Sherbrooke, Quebec J1K 2R1, Canada

Received July 1, 1999

**Abstract:** Properties of the radical anions of three  $\alpha$ -nitrocumenes ( $\alpha$ -nitrocumene, *p*-cyano- $\alpha$ -nitrocumene, and *p*-nitro- $\alpha$ -nitrocumene, **1a–c**) have been determined by electrochemical methods. In particular, the standard potentials of the neutral/radical anion couples were found to be  $-2.20$ ,  $-2.04$ , and  $-1.43$  V with respect to the ferrocenium ion/ferrocene potential and the rate constants for expulsion of nitrite from the radical anions were  $3 \times 10^6$ ,  $5 \times 10^6$ , and  $240 \text{ s}^{-1}$  for **1a–c**, respectively. Comparison of these potentials with those of related compounds demonstrates that reduction of the nitroalkyl portion of the molecule occurs in **1a** and **1b** while in **1c** the electron is added to the nitrophenyl group. Thus, using previously defined terminology, the cleavage of the radical anions of **1a** and **1b** to give nitrite and the corresponding cumyl radicals are examples of homolytic cleavage reactions but the cleavage of the radical anion of **1c** is heterolytic. The driving force for the three cleavage reactions has been estimated and it is concluded that the large decrease in magnitude of the cleavage rate constants on going from **1a** and **1b** to **1c** is mainly due to the much larger driving force for the first two.

## Introduction

The cleavage reaction of radical ions can be classified as homolytic (eq 1a) if the cleavage leaves the charge mainly in the same region as it was in the radical ion or heterolytic (eq 1b) in which there is “regioconservation” of spin density.<sup>2a–e</sup>

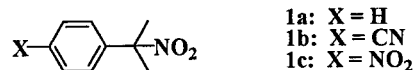


Radical anions are shown in eq 1 as they are the subject of the present paper. Savéant and co-workers have described the heterolytic bond cleavage as an intramolecular dissociative electron transfer in which the electron in an orbital mainly centered on A is transferred to B with concerted bond-breaking.<sup>2f–m</sup> In addition to the systems investigated in the papers cited, other reactions that have been studied include cleavage reactions in the radical anions of  $\alpha$ -aryloxyacetophenones,<sup>3</sup> cleavage of remote C–Br bonds in the radical anions

of benzoate esters,<sup>4</sup> and additional examples in the chloroaromatic family.<sup>5</sup>

Examples of both homolytic and heterolytic bond cleavages in radical ions have been investigated including the effect of variation of substituents so as, for example, to vary the driving force for the cleavage reaction. However, in all cases all members of the family of compounds investigated followed either the homolytic or heterolytic pathway. In the present paper we report the first example of a change in mechanism that occurs when substituents are varied.

The compounds that were studied are the  $\alpha$ -nitrocumenes **1**. The radical anions of the parent compound **1a** and the cyano derivative **1b** undergo homolytic bond cleavage giving nitrite and the corresponding cumyl radical. By contrast, nitro derivative **1c** follows the heterolytic pathway giving the same products.



The electrochemical reduction of **1a** has previously been investigated<sup>6</sup> and it was found that cleavage of nitrite from its radical anion was very rapid, its half-life being  $<1$  ms. Nitrocumene **1a** has also been used as a test reagent to distinguish between electronation–protonation or electrocatalytic hydrogenation mechanisms in the reduction of nitro

(1) (a) University of Delaware. (b) Université de Sherbrooke.  
(2) (a) Maslak, P.; Narvaez, J. N. *Angew. Chem., Int. Ed. Engl.* **1990**, *29*, 283–285. (b) Maslak, P.; Vallombroso, T. M.; Chapman, W. H.; Narvaez, J. N. *Angew. Chem., Int. Ed. Engl.* **1994**, *33*, 73–75. (c) Maslak, P.; Narvaez, J. N.; Vallombroso, T. M. *J. Am. Chem. Soc.* **1995**, *117*, 12373–12379. (d) Maslak, P.; Chapman, W. H., Jr.; Vallombroso, T. M., Jr.; Watson, B. R. *J. Am. Chem. Soc.* **1995**, *117*, 12380–12389. (e) Maslak, P.; Theroff, J. *J. Am. Chem. Soc.* **1996**, *118*, 7235–7236. (f) Savéant, J. M. *Acc. Chem. Res.* **1993**, *26*, 455–461. (g) Savéant, J. M. *J. Phys. Chem.* **1994**, *98*, 3716–3724. (h) Savéant, J. M. *Tetrahedron* **1994**, *50*, 10117–10165. (i) Andrieux, C. P.; Robert, M.; Savéant, J. M. *J. Am. Chem. Soc.* **1995**, *117*, 9340–9346. (j) Andrieux, C. P.; Savéant, J. M.; Tallec, A.; Tardivel, R.; Tardy, C. *J. Am. Chem. Soc.* **1996**, *118*, 9788–9789. (k) Anne, A.; Fraona, S.; Moiroux, J.; Savéant, J. M. *J. Am. Chem. Soc.* **1996**, *118*, 3938–3945. (l) Andrieux, C. P.; Savéant, J. M.; Tallec, A.; Tardivel, R.; Tardy, C. *J. Am. Chem. Soc.* **1997**, *119*, 2420–2429. (m) Andrieux, C. P.; Savéant, J. M.; Tardy, C. *J. Am. Chem. Soc.* **1998**, *120*, 4167–4175.

(3) (a) Andersen, M. L.; Mathivanan, N.; Wayner, D. D. M. *J. Am. Chem. Soc.* **1996**, *118*, 4871–4879. (b) Andersen, M. L.; Long, W.; Wayner, D. D. M. *J. Am. Chem. Soc.* **1997**, *119*, 6590–6595. (c) Andersen, M. L.; Wayner, D. D. M. *Acta Chem. Scand.* In press.  
(4) Antonello, S.; Maran, F. *J. Am. Chem. Soc.* **1998**, *120*, 5713–5722.  
(5) (a) Jaworski, J. S.; Leszczynski, P.; Tykarski, J. *J. Chem. Res., Synop.* **1995**, 510–511. (b) Jaworski, J. S.; Leszczynski, P. *J. Electroanal. Chem.* **1999**, *464*, 259–262.  
(6) Hoffmann, A. K.; Hodgson, W. G.; Maricle, D. L.; Jura, W. H. *J. Am. Chem. Soc.* **1964**, *86*, 631–639.

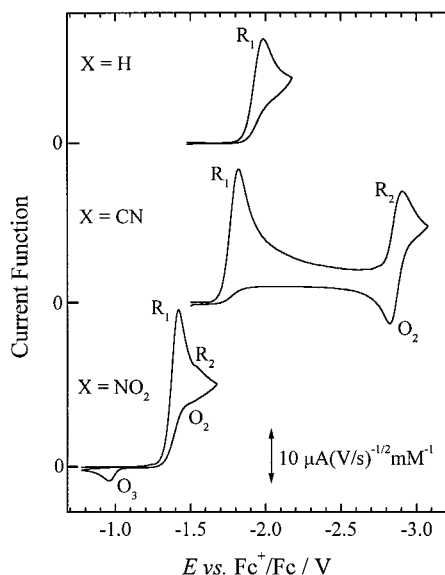
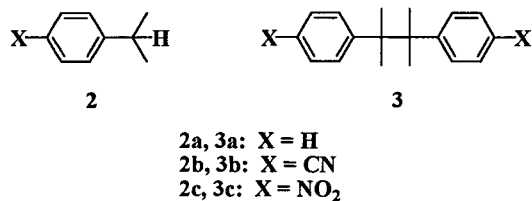


**Figure 1.** Cyclic voltammograms of  $\alpha$ -nitrocumenes **1a–c**. All voltammograms obtained in acetonitrile with 0.10 M Et<sub>4</sub>NClO<sub>4</sub> supporting electrolyte. Working electrode: hanging mercury drop electrode (0.0090 cm<sup>2</sup>). Current function is  $I/v^{1/2}c^*$  where  $I$  is the current,  $v$  the scan rate, and  $c^*$  the concentration. **1a** (X = H):  $v = 1.00$  V/s;  $c^* = 1.00$  mM. **1b** (X = CN):  $v = 1.00$  V/s;  $c^* = 1.02$  mM. **1c** (X = NO<sub>2</sub>):  $v = 0.100$  V/s;  $c^* = 1.08$  mM.

compounds at Raney metal electrodes.<sup>7</sup> In that work, high yields of bicumyl were obtained from reduction of **1a** in basic ethanol–water at mercury electrodes.

## Results

**Cyclic Voltammetry.** Presented in Figure 1 are typical voltammograms for **1a–c** obtained with a mercury electrode in acetonitrile containing 0.10 M Et<sub>4</sub>NClO<sub>4</sub>. The first reduction peak for each compound, R<sub>1</sub>, is an overall two-electron process that is irreversible and diffusion controlled. For **1a** (X = H) no additional reduction peaks were seen in scans to  $-3.1$  V but for **1b** (X = CN) a reversible couple (R<sub>2</sub>/O<sub>2</sub>) appears with  $E^\circ$  equal to  $-2.87$  V.<sup>8</sup> This potential is identical with that found for reduction of *p*-cyanocumene, **2b**. It is possible, however, that the bicumyl (**3b**) would be reduced at about the same potential. The voltammogram of the nitro derivative, **1c**, contains



an analogous but barely detectable R<sub>2</sub>/O<sub>2</sub> pair that in this case

(7) Soazara Chan-Shing, E.; Boucher, D.; Lessard, J. *Can. J. Chem.* **1999**, *77*, 687–694.

(8) (a) What was actually measured was the half-wave potential,  $E_{1/2}$ , which is midway between the cathodic and anodic peak potentials,  $E_{pc}$  and  $E_{pa}$ , respectively.  $E_{1/2} = (E_{pc} + E_{pa})/2$ . The half-wave potential differs from the formal potential,  $E^\circ$ , by a term involving the diffusion coefficients of reactant and product.<sup>8b</sup> Because diffusion coefficients of reactants and products are quite similar, this term is usually less than 10 mV.<sup>8c</sup> We also neglect any differences between the formal potential and the standard potential and will simply refer to our measured value as  $E^\circ$ .<sup>8c</sup> (b) Bard, A. J.; Faulkner, L. R. *Electrochemical Methods. Fundamentals and Applications*; Wiley: New York, 1980; pp 160 and 218–229. (c) See, for example: Lehmann, M. W.; Evans, D. H. *J. Phys. Chem. B* **1998**, *102*, 9928–9933.

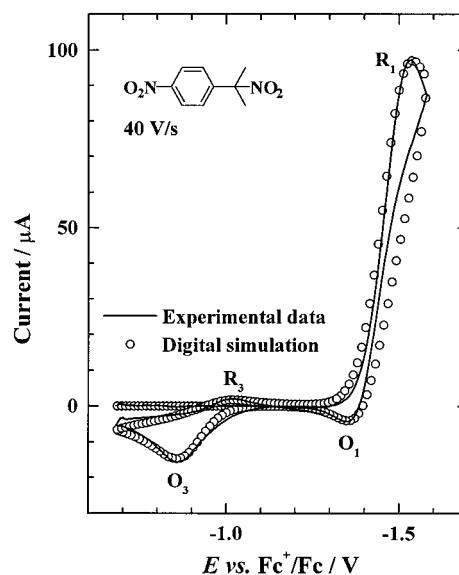


**Figure 2.** Cyclic voltammogram (full curve) of 1.08 mM **1c** at 40 V/s. Other conditions as in Figure 1. Symbols: Digital simulation with  $E^\circ_{1,1c} = 1.43$  V,  $k_{s1,1c} = 0.07$  cm/s,  $\alpha_{1,1c} = 0.5$ ,  $k_{2,1c} = 240$  s<sup>-1</sup>,  $E^\circ_{3,1c} = -0.95$  V,  $k_{s3,1c} = 0.05$  cm/s,  $\alpha_{3,1c} = 0.5$ ,  $k_{4,1c} = 10^8$  M<sup>-1</sup> s<sup>-1</sup>, and  $k_{6,1c} = 2 \times 10^6$  M<sup>-1</sup> s<sup>-1</sup>.  $k_s$  and  $\alpha$  are the standard heterogeneous electron-transfer rate constant and transfer coefficient of the indicated reactions. The values of  $k_s$  must be regarded as approximate due to uncertainties in accounting for the effect of solution resistance. The chemical reactions are regarded as irreversible,  $k_{-2,1c} = 10^{-8} k_{2,1c}$  and  $k_{-6,1c} = 10^{-8} k_{6,1c}$ . All diffusion coefficients were  $2.5 \times 10^{-5}$  cm<sup>2</sup>/s.

is only about 200 mV negative of the main reduction peak. The voltammogram for **1c** was recorded at 0.10 V/s. At higher scan rates, the R<sub>2</sub>/O<sub>2</sub> peaks disappear completely. However, they are distinctly more prominent when DMF is used as solvent. Again, it was found that *p*-nitrocumene, **2c**, gives a reversible set of peaks with the same  $E^\circ$  as the R<sub>2</sub>/O<sub>2</sub> pair,  $-1.52$  V.

The initial electron transfer to the nitrocumenes is rate limiting. Studies of the dependence of the cathodic peak potential of **1a** at glassy carbon on the scan rate lead to a transfer coefficient of 0.46 and a value of 0.53 is found from the peak width.

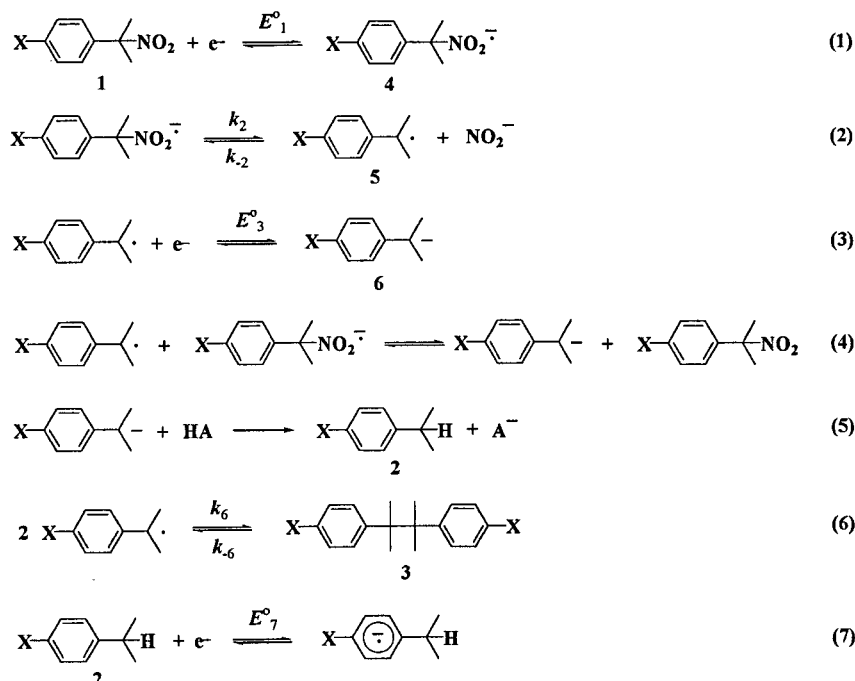
On the return sweep of voltammograms of **1a**, peaks are seen that are associated with oxidation of mercury facilitated by anionic species such as hydroxide that is generated by attack on residual water by strong bases generated in the reduction step.<sup>9</sup> These peaks are absent when a platinum or glassy carbon electrode is used but there is a prominent irreversible anodic peak that occurs at the same potential as seen for a solution of sodium nitrite ( $E_{pa} = +0.12$  V), strong evidence that nitrite is being produced in peak R<sub>1</sub>.

The positive-going sweep in the voltammogram of the cyano derivative, **1b**, also shows only the nitrite oxidation peak at ordinary scan rates. However, when the scan rate was increased to around 1000 V/s (gold microelectrode), a new peak grew in at about  $-1.4$  V which was assigned to the oxidation of the cyanocumyl anion, **6b**, to the corresponding radical, **5b** (Scheme 1).

For the nitro derivative, **1c**, the anodic peak for oxidation of the anion **6c** near  $-1.0$  V is easily detected even at a scan rate of 0.10 V/s, a fact attributable to the lower basicity of **6c** compared to **6b**. In fact, at faster scan rates it is possible to detect some reversibility for the **6c/5c** couple (Figure 2) and thus to determine the standard potential,  $E^\circ_{3c}$ , and the rate

(9) Hu, K.; Niyazymbetov, M. E.; Evans, D. H. *J. Electroanal. Chem.* **1995**, *396*, 457–464.

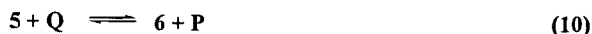
## Scheme 1



constant for the presumed dimerization of the cumyl radicals,  $k_{6c}$  (Table 1).

Also apparent in Figure 2 is a small oxidation peak ( $O_1$ ) that is assigned to the oxidation of the radical anion **4c** to the starting material, **1c**. Fit of the voltammogram by digital simulation allows the determination of the standard potential for the **1c/4c** couple ( $E^{\circ}_{1c}$ ) as well as the rate constant for cleavage of nitrite from **4c**,  $k_2$  (Table 1). By contrast, it was not possible to observe such  $O_1$  oxidation peaks for **1a** and **1b**, even at scan rates as large as 5000 V/s meaning that  $k_2$  must exceed about  $10^4 \text{ s}^{-1}$ .<sup>10</sup>

**Redox Catalysis.** To determine values of  $E^{\circ}_1$  and  $k_2$  for the parent and cyano derivatives, **1a** and **1b**, the technique of homogeneous redox catalysis was applied.<sup>11</sup> To review briefly, a catalyst couple (**P/Q**) is selected that features a reversible electron-transfer reaction with both oxidized and reduced species being stable on the voltammetric time scale. The standard potential,  $E^{\circ}_{PQ}$ , should be less negative than that of the subject of study, in this case  $E^{\circ}_1$ . When both **P** and **1** are present in solution, the reduction peak current for **P** will be enhanced due to the catalytic sequence of reactions 8, 9, 2, and 10. By



measuring the enhanced peak current for reduction of **P** at various concentrations of **1** and **P** and various scan rates, it is possible by means of working curves to evaluate  $k_9$  for the case where forward electron-transfer reaction 9 is rate limiting. In another extreme, reaction 9 can act as a pre-equilibrium step

(10) (a) Nicholson, R. S.; Shain, I. *Anal. Chem.* **1964**, *36*, 706–723. (b) Nicholson, R. S.; Shain, I. *Anal. Chem.* **1965**, *37*, 178–190.

(11) (a) Andrieux, C. P.; Blocman, C.; Dumas-Bouchiat, J. M.; M'Halla, F.; Savéant, J. M. *J. Electroanal. Chem.* **1980**, *113*, 19–40. (b) Savéant, J. M.; Su, K. B. *J. Electroanal. Chem.* **1985**, *196*, 1–22. (c) Andrieux, C. P.; Hapiot, P.; Savéant, J. M. *Chem. Rev.* **1990**, *90*, 723–738. (d) Nadjio, L.; Savéant, J. M.; Su, K. B. *J. Electroanal. Chem.* **1985**, *196*, 23–34.

**Table 1.** Summary of Results for the  $\alpha$ -Nitrocumenes **1a–c**

quantity	$\alpha$ -nitro-cumene, <b>1a</b>	<i>p</i> -cyano- $\alpha$ -nitro-cumene, <b>1b</b>	<i>p</i> -nitro- $\alpha$ -nitro-cumene, <b>1c</b>
$E^{\circ}_1/\text{V vs Fc}^+/\text{Fc}$	-2.20	-2.04	-1.43
$\alpha_1^a$	0.59	0.46	
$k_2/\text{s}^{-1}$	$3 \times 10^6$	$5 \times 10^6$	240
$E^{\circ}_3/\text{V vs Fc}^+/\text{Fc}$	$\approx -1.9^c$	$\approx -1.4^b$	-0.94
$k_6/\text{M}^{-1}\text{s}^{-1}$			$2 \times 10^6$
$E^{\circ}_7/\text{V vs Fc}^+/\text{Fc}$	-3.8 <sup>d</sup>	-2.87	-1.52

<sup>a</sup> From dependence of peak potential on scan rate,  $\alpha = (RT/2F)/(dE_{p,R1}/d \ln v)$ . <sup>b</sup> Irreversible peak potential for oxidation of the *p*-cyanocumyl anion at fast scan rate. <sup>c</sup> Estimated from fits of digital simulation to voltammograms with "total catalysis", Figure 3, for example. <sup>d</sup> Assumed to be the same as for the reduction of benzene in dimethoxyethane.<sup>21</sup>

and the catalysis will be governed completely by the cleavage reaction 2 permitting evaluation of  $k_2$  if  $K_9$  is known by virtue of knowing  $E^{\circ}_{PQ}$  and  $E^{\circ}_1$ . In other situations, the system is under mixed control by reactions 9 and 2.<sup>11</sup> In some cases it is necessary to consider the coupling reaction of **5** with **Q** but our experiments were performed under conditions (small ratio of the concentration of **1** to that of **P**) where there is no significant effect of such a coupling reaction on the evaluated rate constants.<sup>11d</sup>

Compounds **1a** and **1b** were investigated using a variety of catalysts for which the overall reaction was under control of forward electron-transfer reaction 9 allowing the determination of  $k_9$ . The results are summarized in Table 2. It is expected that plots of  $\log k_9$  vs the standard potential of the catalysts will be linear with slopes of  $1/0.0592 \text{ V}^{-1}$  as long as the back reaction is diffusion controlled,  $k_{-9} = k_{\text{dif}}$ . (The diffusion-controlled rate constant,  $k_{\text{dif}}$ , has been estimated to be  $10^{10} \text{ M}^{-1} \text{ s}^{-1}$  using procedures described elsewhere.<sup>12</sup>) Extrapolation of such linear plots allows the determination of  $E^{\circ}_1$ , the potential at which  $\log k_9$  equals  $\log k_{\text{dif}}$ .<sup>13</sup>

(12) (a) Kojima, H.; Bard, A. J. *J. Am. Chem. Soc.* **1975**, *97*, 6317–6324. (b) Oliver, E. W.; Evans, D. H. *J. Electroanal. Chem.* **1997**, *432*, 145–151.

(13) Andrieux, C. P.; Blocman, C.; Dumas-Bouchiat, J. M.; Savéant, J. M. *J. Am. Chem. Soc.* **1979**, *101*, 3431–3441.

**Table 2.** Results of Homogeneous Redox Catalysis

catalyst	$E^\circ/\text{V}$	$k_9/\text{M}^{-1}\text{s}^{-1}$
<i><math>\alpha</math>-nitrocumene<sup>a</sup></i>		
2,3-dimethylnitrobenzene	-1.694	28
2-methoxynitrobenzene	-1.696	31
2,4-dimethylnitrobenzene	-1.706	59
azobenzene	-1.775	680
<i><math>p</math>-cyano-<math>\alpha</math>-nitrocumene<sup>b</sup></i>		
nitrobenzene	-1.545	51
benzil	-1.560	85
4-methylnitrobenzene	-1.588	260
4-methoxynitrobenzene	-1.645	950
2-methylnitrobenzene	-1.655	890
2,3-dimethylnitrobenzene	-1.694	1800
2-methoxynitrobenzene	-1.696	1100
2,4-dimethylnitrobenzene	-1.706	1500

<sup>a</sup> Fit to  $\log k_9 = a_0 - E^\circ/0.0592$  gives  $a_0 = -27.15$ . <sup>b</sup> Fit to  $\log k_9 = a_0 - E^\circ/0.0592$  gives  $a_0 = -24.42$  for the first three catalysts. Fit to  $\log k_9 = a_0 - E^\circ/0.1184$  gives  $a_0 = -11.10$  for the last five catalysts.

For **1a**, a linear relationship with slope of  $1/0.0592 \text{ V}^{-1}$  was found leading to  $E^\circ_{1,1a}$  of  $-2.20 \text{ V}$ . In the case of cyano derivative **1b**, only the three catalysts with the least negative potentials gave results with the theoretical slope leading to  $E^\circ_{1,1b}$  of  $-2.04 \text{ V}$ . The data for the five remaining catalysts adhered to a slope of  $1/0.1184 \text{ V}^{-1}$  which is consistent with activation control<sup>13</sup> and gave an extrapolated estimate for the value of  $k_9$  at zero driving force of  $10^6 \text{ M}^{-1} \text{ s}^{-1}$ . This result is 1 to 2 orders of magnitude lower than found for most halobenzenes and halopyridines<sup>13</sup> consistent with the higher activation energy associated with electron transfer to nitroalkanes.<sup>14</sup>

The working curves for the overall two-electron catalyzed reduction of **1a** and **1b** (reactions 8, 9, 2, and 10) were used in the evaluation of the data in Table 2. This requires that the reduced forms of the catalysts be capable of reducing the cumyl radical (reaction 10). This is a reasonable assumption for **1b** because  $E^\circ_{3,1b}$  should be around  $-1.4 \text{ V}$ , as indicated earlier. Thus, for all of the catalysts used in the study of **1b**, reaction 10 will be at least  $0.15 \text{ V}$  downhill and the overall two-electron pathway is reasonable. However, as shown below,  $E^\circ_{3,1a}$  is probably near  $-1.9 \text{ V}$  so reaction 10 is not favored for any of the four catalysts used in the study of **1a**. However, when the working curves for the one-electron mechanism were used, the results were very similar to those shown in Table 2, the extrapolated value of  $E^\circ_{1,1a}$  being  $-2.18 \text{ V}$  compared to  $-2.20 \text{ V}$  from the two-electron analysis. Very rapid protonation of the benzyl anion formed in reaction 10 may be sufficient to drive the slightly uphill reactions ( $0.2\text{--}0.3 \text{ V}$ ) causing the catalysis to proceed by the two-electron mechanism. In any case, evaluation of  $E^\circ_{1,1a}$  depends only very weakly on the choice of mechanism.

For the parent compound **1a** and the catalyst *p*-dimethylaminoazobenzene it was found that "total catalysis" occurred, i.e., the catalysis was so efficient that a prepeak appeared at potentials less negative than the peak for reduction of the catalyst alone (Figure 3).<sup>11a–b</sup> Using the value of  $E^\circ_{1,1a}$  obtained above along with  $E^\circ_{\text{PQ}}$  for *p*-dimethylaminoazobenzene ( $-2.01 \text{ V}$ ) it was possible to fit the voltammograms for various concentrations of catalyst and **1a** as well as various scan rates to obtain  $k_2$ . The result was  $k_{2,1a} = 3 (\pm 2) \times 10^6 \text{ s}^{-1}$ . An example of a fit of simulation to the voltammogram is included in Figure 3. Best

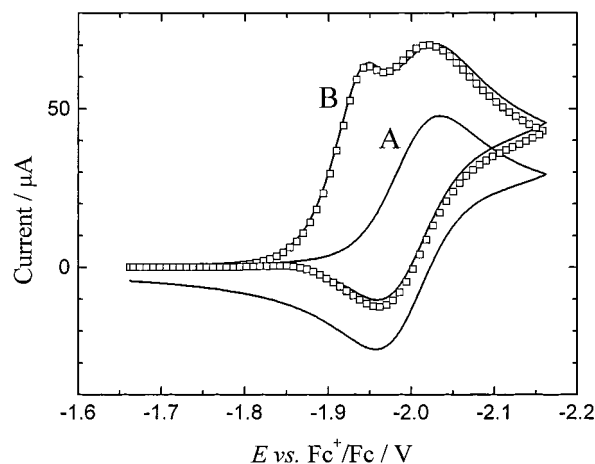


**Figure 3.** Voltammograms showing the reduction of  $\alpha$ -nitrocumene (**1a**) catalyzed by *p*-dimethylaminoazobenzene. Glassy carbon electrode in DMF containing  $0.10 \text{ M Bu}_4\text{NPF}_6$  at  $298 \text{ K}$ . Scan rate:  $0.050 \text{ V/s}$ . Curve A:  $4.00 \text{ mM } p$ -dimethylaminoazobenzene. Curve B: After addition of  $2.00 \text{ mM } \alpha$ -nitrocumene (**1a**). Symbols: Digital simulation with the following parameter values (see reactions 8, 9, 2, and 10 for definitions):  $E^\circ_{\text{PQ}} = -2.01 \text{ V}$ ,  $k_{s,8} = 0.018 \text{ cm/s}$ ,  $\alpha_8 = 0.50$ ,  $K_9 = 8 \times 10^{-4}$ ,  $k_9 = 4 \times 10^6 \text{ M}^{-1} \text{ s}^{-1}$ ,  $K_2 = 10^9 \text{ M}$ ,  $k_2 = 3 \times 10^6 \text{ s}^{-1}$ ,  $K_{10} = 50$ ,  $k_{10} = 4 \times 10^5 \text{ M}^{-1} \text{ s}^{-1}$ , rate constant for irreversible protonation of cumyl anion was  $10 \text{ s}^{-1}$ , all diffusion coefficients set at  $4 \times 10^{-6} \text{ cm}^2/\text{s}$ , and electrode area =  $0.0855 \text{ cm}^2$ . Spherical diffusion was used to mimic edge diffusion to the disk electrode. Most parameter values were fixed at levels determined in separate experiments. For example,  $E^\circ_{\text{PQ}}$  and  $k_{s,8}$  were determined from voltammograms of catalyst alone (like curve A),  $K_9$  was derived from  $E^\circ_{\text{PQ}}$  and  $E^\circ_{1,1a}$  from redox catalysis, and  $k_9$  was obtained by extrapolation of the results of redox catalysis for other catalysts. The adjustable parameters were  $k_2$  and  $K_{10}$  ( $k_{10}$  had little effect unless it was too small) and the best fit value of 50 for  $K_{10}$  leads to a value of  $E^\circ_{3,1a}$  of  $-1.91 \text{ V}$ . DMF was used as a solvent because the P/Q couple was less reversible in acetonitrile.

agreement was achieved when the value of  $E^\circ_{3,1a}$  was about  $-1.90 \text{ V}$ , which suggests, as mentioned above, that reaction 10 is an uphill reaction for the other catalysts used to study **1a** (Table 2).

In the study of **1b** by redox catalysis, it was found that passage to a region of mixed control occurred with one of the catalysts, 2,3-dimethylnitrobenzene. Such a transition is signaled by reduction in the magnitude of  $k_9$  at high catalyst concentration when evaluated using working curves that suppose forward reaction 9 to be rate limiting. For **1b** and catalyst concentrations of  $4 \text{ mM}$  or less, constant values of  $k_9$  were obtained ( $1800 \text{ M}^{-1} \text{ s}^{-1}$ ), but at  $10 \text{ mM}$  the values were significantly smaller. Using the value of  $E^\circ_{1,1b}$  obtained above ( $-2.04 \text{ V}$ ), the value of  $E^\circ_{\text{PQ}}$  ( $-1.694$ ), and eq 11, the value of  $k_{-9}$  can be calculated.

$$\log\left(\frac{k_9}{k_{-9}}\right) = \frac{E^\circ_{1,1b} - E^\circ_{\text{PQ}}}{2.303RT/F} \quad (11)$$

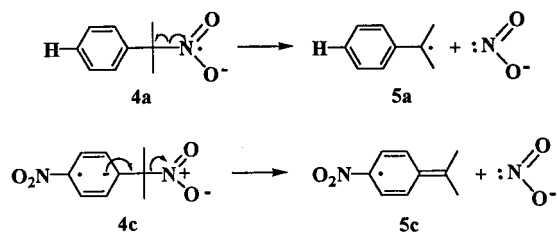
The result is  $k_{-9} = 1.3 \times 10^9 \text{ M}^{-1} \text{ s}^{-1}$ . This allows construction of a working curve of the catalytic peak current as a function of  $k_2$  using the known values of  $k_9$ ,  $k_{-9}$ ,  $E^\circ_{\text{PQ}}$ , and  $E^\circ_{1,1b}$ . When the data obtained at  $10 \text{ mM}$  catalyst were analyzed using this working curve, the average result was  $k_{2,1b} = 5 (\pm 3) \times 10^6 \text{ s}^{-1}$ , identical with that found for **1a**.

## Discussion

What is the basis of the claim made in the Introduction that in the radical anions of **1** there is a transition from homolytic cleavage in **4a** and **4b** to heterolytic in **4c**? The difference

(14) (a) Corrigan, D. A.; Evans, D. H. *J. Electroanal. Chem.* **1980**, *106*, 287–304. (b) Petersen, R. A.; Evans, D. H. *J. Electroanal. Chem.* **1987**, *222*, 129–150. (c) Gilicinski, A. G.; Evans, D. H. *J. Electroanal. Chem.* **1989**, *267*, 93–104. (d) Evans, D. H.; Gilicinski, A. G. *J. Phys. Chem.* **1992**, *96*, 2528–2533.

## Scheme 2



between these pathways is illustrated for **4a** and **4c** by conventional “electron-pushing” diagrams in Scheme 2. In the homolytic cleavage (as for **4a**), the charge is located mainly on the  $\alpha$ -nitro group and it remains there as the cleavage occurs giving nitrite and the cumyl radical. In the heterolytic cleavage (as in **4c**), the charge and spin density are originally associated with the nitrophenyl portion in the radical anion but the charge moves to the leaving nitrite ion leaving the spin density in the nitrophenyl group.

First, it is necessary to demonstrate that the leaving group in all cases is nitrite rather than  $\text{NO}_2$ . One point of evidence is the fact that on the return sweep of cyclic voltammograms of **1a–c** prominent oxidation peaks for nitrite were seen for all three compounds. In addition, the estimated values of  $E^\circ_3$  are all more negative than  $-0.9$  V (Table 1) whereas the estimated potential for the  $\text{NO}_2/\text{NO}_2^-$  couple is  $+0.1$  V (see below). This means that cleavage to nitrite and the cumyl radical is more than 1 V (23 kcal/mol) more favorable than the alternative cleavage to  $\text{NO}_2$  and the cumyl anion.

Next, it must be shown that it is the  $\alpha$ -nitro group that is the site of reduction in **1a** and **1b** whereas it is the nitrophenyl group that receives the electron in **1c**. The simplest and perhaps most persuasive argument supporting this conclusion is based on a comparison of standard potentials. Presented in Figure 4 are the potentials of the neutral/radical anion couples for three types of compounds: (1) three cumenes (*p*-nitrocumene, *p*-cyanocumene, and cumene); (2) the three  $\alpha$ -nitrocumenes studied here, **1a–c**; and (3) nitroalkanes as exemplified by 2-methyl-2-nitropropane.

Starting with **1c**, one can see that its standard potential is very close to that of *p*-nitrocumene but it is about 0.5 V positive of the potential required to reduce a typical nitroalkane. That is, it is clearly the nitrophenyl portion of **1c** that receives the electron and not the nitropropyl group. By contrast, the potentials for **1a** and **1b** are similar to one another and fall in the same region as the standard potential for nitroalkanes. It is much more difficult to insert an electron into the aromatic portion of **1a** and **1b** as shown by the much more negative potentials for *p*-cyanocumene and cumene (estimated). So, for **1a** and **1b** it is the nitropropyl group that receives the electron rather than the aromatic portion of the molecule.

Of course, it is the entire molecule that receives the electron upon reduction and not any isolated portion of it. So the statements above should probably be somewhat modified to indicate that in **1a** and **1b** it is mainly the  $\alpha$ -nitro group that is reduced whereas for **1c** the added electron is mainly associated with the nitrophenyl group.

Finally we will consider the factors that underlie the large differences in the rate constant for cleavage seen for **1a** and **1b** as compared with **1c** (Table 1). In the theory for concerted electron transfer–bond breaking in the cleavage reactions of radical ions,<sup>2e</sup> two factors govern the free energy of activation. They are the intrinsic barrier free energy and the driving force of the reaction. The driving force for bond cleavage can be

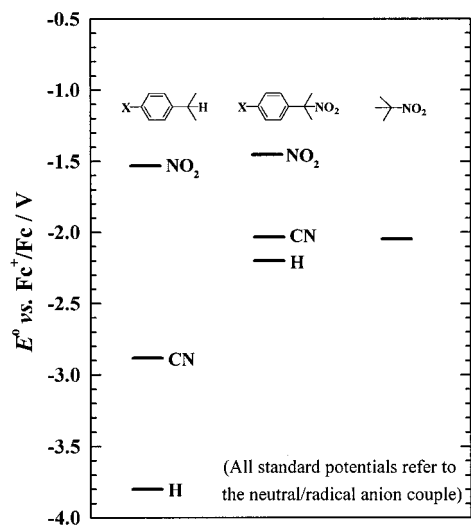


Figure 4. Standard potentials for various couples considered in this work.

estimated from the measured standard potentials and the C–N bond dissociation energy (eq 12).<sup>1g</sup>

$$\Delta G^\circ_2 = D_{\text{RNO}_2} + F(E^\circ_1 - E^\circ_{\text{NO}_2/\text{NO}_2^-}) + T(S^\circ_{\text{RNO}_2} - S^\circ_{\text{R}} - S^\circ_{\text{NO}_2}) \quad (12)$$

Here  $D_{\text{RNO}_2}$  is the C–N bond dissociation energy (considered to be independent of the nature of R) and  $S^\circ_j$  denotes the standard entropy of species *j*. A value of 50 kcal/mol for  $D_{\text{RNO}_2}$  was estimated from bond additivity principles and literature data for the enthalpy of formation of  $\text{NO}_2$ .<sup>15</sup> Values for  $S^\circ_{\text{RNO}_2}$  (107 cal mol<sup>-1</sup> K<sup>-1</sup>) and  $S^\circ_{\text{R}}$  (110 cal mol<sup>-1</sup> K<sup>-1</sup>) were the same as those used for *p*-nitrocumyl chloride<sup>16</sup> while the value for  $\text{NO}_2$  (57 cal mol<sup>-1</sup> K<sup>-1</sup>) was taken from the literature.<sup>15b</sup> Finally,  $E^\circ_{\text{NO}_2/\text{NO}_2^-}$  was estimated to be  $+0.10 \pm 0.05$  V based on its value in water<sup>17</sup> and the assumption that the free energy of transfer of nitrite from water to acetonitrile is the same as that of bromide.<sup>2g</sup> This estimate for  $E^\circ_{\text{NO}_2/\text{NO}_2^-}$  is identical with the irreversible peak potential for oxidation of nitrite mentioned earlier.

Taking the values of  $E^\circ_1$  for **1a–c** (Table 1), we obtain free energies of cleavage of radical anions **4a–c** of  $-21$ ,  $-18$ , and  $-4$  kcal/mol for the parent compound, the cyano derivative, and the nitro derivative, respectively. Thus there is a substantial difference in driving force between **4a** and **4b**, on one hand, and **4c**, on the other, and we may conclude that it is principally this difference in the free energy of the cleavage reaction that underlies the difference in rate constants of 4 orders of magnitude. A more detailed analysis would entail calculation of the intrinsic barrier for the cleavage reaction, a calculation that requires knowledge of the energy of certain excited states

(15) (a) As a test of accuracy, the bond additivity relationships<sup>15b</sup> were used to calculate the standard enthalpy of formation of 2-nitropropane and 2-methyl-2-nitropropane. These were in turn combined with the enthalpy of formation of  $\text{NO}_2$ <sup>15c</sup> and those of isopropyl and *tert*-butyl radicals<sup>15d</sup> to obtain predicted bond dissociation energies. These were found to be 3–5 kcal/mol larger than experimental.<sup>15d</sup> The same procedure applied to  $\alpha$ -nitrocumene gave a bond dissociation energy of 54 kcal/mol that was adjusted to 50 kcal/mol in view of the above calculations with the two nitroalkanes. (b) Benson, S. W. *Thermochemical Kinetics*; Wiley: New York, 1976. (c) *CRC Handbook of Chemistry and Physics*, 76th ed.; Lide, D. R., Ed.; CRC Press: Boca Raton, FL, 1995; pp 5–19. (d) McMillen, D. F.; Golden, D. M. *Annu. Rev. Phys. Chem.* **1982**, *33*, 493–532.

(16) Costentin, C.; Hapiot, P.; Médebielle, M.; Savéant, J. M. *J. Am. Chem. Soc.* **1999**, *121*, 4451–4460.

(17) Wardman, P. *J. Phys. Chem. Ref. Data* **1989**, *18*, 1637–1755.

of the cumyl anion for heterolytic cleavage and of nitrite for homolytic cleavage.<sup>2g</sup>

## Experimental Section

**Instrumentation and Procedures.** Standard electrochemical cells, electrodes, and instrumentation were employed. Unless otherwise specified, an EG&G Princeton Applied Research Model 303A static mercury drop electrode (small size drop) was used in cyclic voltammetric studies and a 3.3-mm diameter glassy carbon disk electrode was used for redox catalysis. For fast-scan cyclic voltammetry, a 50- $\mu$ m diameter gold disk microelectrode was used. The laboratory reference electrode comprised a silver wire in contact with 0.010 M AgNO<sub>3</sub>, 0.10 M Bu<sub>4</sub>NPF<sub>6</sub> in acetonitrile. The standard potential for the ferrocenium ion/ferrocene couple was frequently measured with respect to the laboratory reference and all potentials reported herein are with respect to the ferrocene potential. The experiments were conducted at room temperature.

Digital simulations were performed with the software package DigiSim (Bioanalytical Systems, version 2.1).

**Chemicals.** Optima grade acetonitrile (Fisher) was used as received. *N,N*-Dimethylformamide was dried with anhydrous MgSO<sub>4</sub>, distilled under reduced pressure, and passed through a column of activated alumina before use. Electrolytes were purified according to standard methods, and all reagents and catalysts were of commercial origin and were used as received except for *p*-dimethylaminoazobenzene which was recrystallized from 95% ethanol.

**$\alpha$ -Nitrocumene, 1a.**  $\alpha$ -Nitrocumene was prepared according to the literature<sup>6</sup> by the reaction of diphenyliodonium chloride with 2-nitropropane and potassium *tert*-butoxide. The product obtained after vacuum distillation was slightly yellow but passage through a short column of alumina produced a colorless liquid. <sup>1</sup>H NMR (CDCl<sub>3</sub>)  $\delta$  (ppm) 1.98 (s, 6H), 7.37 (m, 5H).

***p*-Cyano- $\alpha$ -nitrocumene, 1b.** First, 2-nitropropane was reacted with lithium wire in absolute methanol to produce the lithium salt of

2-nitropropane.<sup>18</sup> This salt was reacted with *p*-nitrobenzocyanide according to the literature<sup>19</sup> and the product was chromatographed on silica gel using benzene/petroleum ether (3:1) as eluent and finally recrystallized from pentane, mp 59–60 °C; <sup>1</sup>H NMR (CDCl<sub>3</sub>)  $\delta$  (ppm) 2.0 (s, 6H), 7.5 (d, 2H), 7.7 (d, 2H).

***p*-Nitro- $\alpha$ -nitrocumene, 1c.** This derivative was obtained from  $\alpha$ -bromo-*p*-nitrocumene (itself prepared by reaction of *p*-nitrocumene with *N*-bromosuccinimide) and sodium cyanide in DMF at 25 °C for 48 h following Kornblum's method.<sup>20</sup> The product was recrystallized twice from methanol, mp 66.5–68 °C; <sup>1</sup>H NMR (CDCl<sub>3</sub>)  $\delta$  (ppm) 2.0 (s, 6H), 7.6 (d, 2H), 8.2 (d, 2H).

***p*-Cyanocumene.** A solution of 3.54 g of the oxime of 4-isopropylbenzaldehyde (prepared by reaction of 4-isopropylbenzaldehyde with hydroxylamine hydrochloride in pyridine and anhydrous ethanol) in 25 mL of acetic anhydride was refluxed for 4 h. To the cooled solution was added 0.6 g of P<sub>2</sub>O<sub>5</sub> and the reflux was continued for another 30 min. After cooling, the solution was poured into 50 mL of water and extracted with ether (3 $\times$ ). After drying with MgSO<sub>4</sub>, the ether was evaporated and the residue was distilled under vacuum giving 2.5 g of *p*-cyanocumene. <sup>1</sup>H NMR (CDCl<sub>3</sub>)  $\delta$  (ppm) 2.4 (d, 6H), 2.9 (m, 1H), 7.3 (d, 2H), 7.5 (d, 2H).

**Acknowledgment.** This work was supported by the National Science Foundation, Grant CHE-9704211.

JA9922779

(18) Kornblum, N.; Boyd, S. D.; Ono, N. *J. Am. Chem. Soc.* **1974**, *96*, 2580–2587.

(19) Kornblum, N.; Cheng, L.; Kerber, R. C.; Kestner, M. M.; Newron, B. N.; Pinnick, H. W.; Smith, R. G.; Wade, P. A. *J. Org. Chem.* **1976**, *41*, 1560–1564.

(20) Kornblum, N.; Davies, T. M.; Earl, G. W.; Holy, N. L.; Kerber, R. C.; Musser, M. T.; Snow, D. H. *J. Am. Chem. Soc.* **1967**, *89*, 725–727.

(21) Mortensen, J.; Heinze, J. *Angew. Chem., Int. Ed. Engl.* **1984**, *23*, 84–85.